Proceedings of ASME Turbo Expo 2020
Turbomachinery Technical Conference and Exposition
GT2020
June 22-26, 2020, London, England

GT2020-14581

INDUSTRIAL WASTEWATER AS AN ENABLER OF GREEN AMMONIA TO POWER VIA GAS TURBINE TECHNOLOGY

S. G. Hewlett*, D. G. Pugh, A. Valera-Medina, A. Giles, J. Runyon, B. Goktepe, P.J. Bowen.
Cardiff University School of Engineering,
Cardiff, Wales, UK, CF24 3AA.
Email: hewlettsg4@cardiff.ac.uk, valeramedinaa1@cardiff.ac.uk

ABSTRACT

This experimental study follows on from detailed Chemkin-Pro numerical analyses assessing the viability of by-product ammonia (NH_3) utilization for power generation in gas turbines (GTs). This study looks specifically at NH_3 in the industrial wastewaters of steelworks, resulting from the cleansing of coke oven gas (COG). The by-product NH_3 is present in an aqueous blend of 60-70%$_{vol}$ water and is normally destroyed.

An experimental campaign was conducted using a premixed swirl burner in a model GT combustor, previously employed in the successful combustion of NH_3/hydrogen blends, with favorable NO_x and unburned fuel emissions. This study experimentally investigates the combustion performance of combining anhydrous and aqueous by-product NH_3 in an approximate 50:50%$_{vol}$ blend, comparing the performance with that of each ammonia source unblended. Green anhydrous NH_3, a rapidly growing research topic, is a carbon-free energy vector for renewable hydrogen. Some potential benefits of combining the two sources are suggested.

Ammonia combustion presents two major challenges, poor reactivity and a potential for excessive NO_x emissions. Prior numerical analyses predicted that 15%$_{vol}$ addition of steelworks COG, at an inlet temperature of 550 K, may provide sufficient support for raising the reactivity of the NH_3-based fuels, whilst limiting undesirable emissions. Therefore, addition of 10, 15 and 20%$_{vol}$ COG to each NH_3-based fuel was investigated experimentally at 25 kW power with inlet temperatures > 500 K, at atmospheric pressure.

As nitric oxide (NO) emissions decrease significantly with increasing fuel-to-air ratio, experiments were conducted at equivalence ratios (Φ) between 1.0 and 1.3, the precise range of Φ for each blend being optimized according to the modeling predictions for emissions. Leading blends, anhydrous NH_3 with 15%$_{vol}$ COG and the 50:50%$_{vol}$ blend with 15%$_{vol}$ COG, achieved < 100 ppm and < 200 ppm NO respectively.

Modest-sized steel plants produce ~10 metric tons of by-product NH_3/day. Aspen Plus was used to model a Brayton-Rankine cycle with integrated recuperation. Adopting typical losses (48% cycle efficiency) and ~1.2 MPa combustor inlet pressure, the net electrical power generation of 15%$_{vol}$ COG blended with 10 tonnes/day of aqueous industrial NH_3 and 25 tonnes/day of anhydrous NH_3 (i.e. achieving a 50:50%$_{vol}$ blend) was ~4.7 MW, ~47% more power than for the same amount of anhydrous NH_3 with 15%$_{vol}$ COG. This significant increase, indicates how industrial NH_3 could enable green NH_3 to power.

Keywords: Ammonia, Gas Turbine, Industrial Wastewater, Swirl Flame, NO Emissions

NOMENCLATURE

AA	Anhydrous Ammonia
AFT	Adiabatic Flame Temperature
AqAV	Aqueous Ammonia Vapor
COG	Coke Oven Gas
GT	Gas Turbine
HRSG	Heat Recovery Steam Generator
LHV	Lower Heating Value
MFC	Mass Flow Controller
Φ	Equivalence Ratio
S_L	Laminar Flame speed

*Address all correspondence to this author

1. INTRODUCTION

This study investigates the potential for combining green ammonia, a carbon-free, renewably-produced hydrogen energy vector, with waste-stream ammonia found in industrial wastewaters, for power generation via gas turbines (GT).

1.1 Green ammonia

Hydrogen produced via the electrolysis of water using renewable electricity is termed green hydrogen. Pure, anhydrous ammonia (AA) manufactured using a green hydrogen feed and nitrogen from air, is termed green ammonia. When green ammonia is used to generate power, the cycle from power-to-gas-to-power is completed. In this manner, green ammonia is considered a potential enabler for the deployment of renewable hydrogen [1–3].

The conversion of hydrogen to ammonia is energy intensive, requiring 7.8 MWh of energy per metric ton (tonne) under best practice, using natural gas [4]. Despite the energy intensity of production, the conversion is favored due to the modest conditions required for ammonia's storage and transport. Anhydrous ammonia can be stored as a liquid at a modest pressure of ~0.8 MPa at 293 K [1], or below 240 K at atmospheric pressure. By contrast, liquefying hydrogen requires a temperature of 20 K at atmospheric pressure [5, 6], yet the hydrogen density of liquid hydrogen is still considerably lower than that of liquid ammonia, as shown in Fig.1.

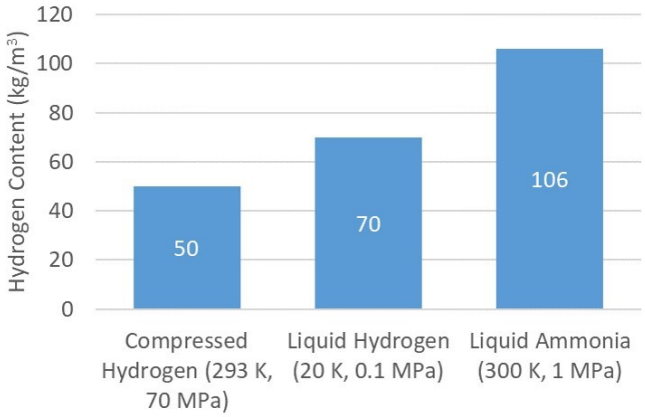

FIGURE 1. HYDROGEN DENSITIES OF AMMONIA AND HYDROGEN UNDER VARYING CONDITIONS [5, 6].

With a global trade in 2018 of approximately 140 Mt (nitrogen equivalent) [7], ammonia has large scale, established transport and handling networks, unlike hydrogen. When comparing with other liquid fuels, AA has a lower heating value (LHV) of 18.6 MJ/kg, similar to methanol and half that of diesel.

1.2 By-product ammonia

In contrast to the energy intensive production of ammonia, many industrial waste streams contain significant amounts of unwanted and readily available by-product ammonia. These industrial wastewaters could be used to augment the ammonia available from renewable sources, thus encouraging earlier and larger scale development of the infrastructure required to generate power from ammonia-based fuels.

Many industries handling material of organic origin have ammonia and hydrogen sulfide (H_2S) in their material flows. Obvious examples include agriculture, sewage treatment and biomass gasification. Fossil fuels are also of organic origin, so coal carbonization and oil refining have significant aqueous waste streams, termed sour waters, containing these two impurities.

This paper focuses on ammonia waste streams in the steel industry for two main reasons. First, coke is a reductant and fuel source in the blast furnace and the carbonization of coal to coke produces a particularly concentrated ammonia waste stream of ~3 kg per tonne of coke [8]. The ammonia is captured during the cleansing of coke oven gas (COG), the volatile component of coal [9]. Secondly, crude steel manufacture using a blast furnace produces pig iron. After the blast furnace, the basic oxygen furnace decarbonizes pig iron with oxygen, during its conversion to steel. This oxygen is sourced via air separation, resulting in a nitrogen by-product, locally available for green or other ammonia manufacture. Although this study considers green ammonia as a source of AA, ammonia can also be produced with hydrogen obtained from COG [9]. This could be of particular interest in China, where 49% of global crude steel is produced, 91% via blast furnaces [10] and where, in 2013, only 20% of COG was reported as being utilized as fuel [11].

COG is composed predominantly of hydrogen (~60%$_{vol}$), methane (~24%$_{vol}$) and carbon monoxide (~7%$_{vol}$) [8, 12]. In volumetric terms, COG has a higher heating value of 17-18 MJ/Nm^3 [8, 12, 13], around half that of methane. Raw COG is laden with impurities, including NH_3 and H_2S in similar concentrations [8]. Under typical coke oven processing conditions (i.e. ≥ 1200 K), ammonia in COG constitutes around 10-15% of all the nitrogen originally present in the coal [9].

Ammonia presents a serious threat to human health and the environment when poorly managed. Ammonia is a toxic and corrosive substance and is especially dangerous to aquatic environments. Therefore, it is necessary to remove ammonia and other contaminants from COG before utilization as a fuel.

NH_3 and H_2S dissolve readily in water. Therefore, COG cleansing processes conventionally use water to strip the NH_3 and H_2S from COG. The processing produces an ammonia-rich waste stream which undergoes a final stage of recovery or destruction. This stream is maintained as a vapor at ~360 K and has a typical composition as shown in Fig. 2 [13, 14]. The ammonia-rich stream in Fig. 2 has a LHV of 6.8 MJ/kg and will henceforth be referred to as aqueous ammonia vapor (AqAV), to concisely differentiate it from AA.

Approximately 450 to 480 kg of coke is consumed for every tonne of steel produced, generating ~1.5 kg of ammonia, [15, 16]. Therefore, a modest sized integrated steelworks (e.g. 2.7 Mt steel per annum) will produce in excess of 3,500 tonnes of ammonia from its coke ovens each year, equivalent to approximately 10 tonnes per day. Consequently, the steel industry has a long history of managing by-product ammonia.

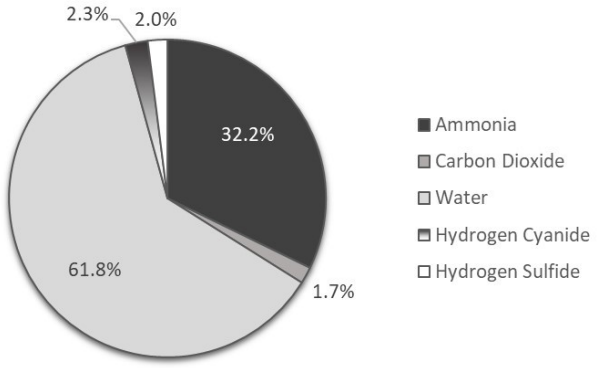

FIGURE 2. TYPICAL COMPOSITION ($\%_{VOL}$) OF STEELWORKS AQUEOUS AMMONIA VAPOR (AqAV) [13, 14]

Several methods can be used to recover, rather than destroy the ammonia. These include reacting with sulfuric acid to produce ammonium sulfate fertilizer and the PHOSAM process for the recovery of >99% purity AA [9, 14]. Currently ~72% of global ammonia is produced via the Haber-Bosch process, utilizing hydrogen from natural gas [4]. In comparison to this large-scale process, ammonia recovery from industrial wastewater is uneconomical, resulting in moves to destroy rather than recover the ammonia, either through its catalytic destruction or incineration. These market conditions could of course change if CO_2 emissions, from the use of natural gas (~1.6 tonnes per tonne of AA [4]), were costed to significantly impair the economics of producing synthetic ammonia.

Energy recovery from the destruction of industrial by-product ammonia is not a legal requirement in the European Union [8]. While heat recovery from the destruction of industrial AqAV is often practiced [13, 14, 17], no evidence has been found of direct combustion of AqAV in GT, or any other type of power generation technology. GT combustion of AA on the other hand, was first investigated in the 1960s [18] and with recent interest in power-to-gas-to-power via green ammonia, research in this field has undergone a recent surge in activity [19–26].

1.3 Ammonia combustion

Two major challenges encountered when utilizing ammonia as a fuel are its comparatively low reactivity [18] and the potential for very high exhaust NO_x concentrations [27]. Characteristics of low reactivity include low laminar burning velocity (S_L), high minimum ignition energy and narrow flammability range. These poor combustion characteristics are especially problematic when using existing GT technology designed for use with conventional fuels. The reactivity of AqAV is naturally considerably poorer than for AA, given the substantial water component (~$60\%_{vol}$).

One method used to address the issue of low reactivity is to use more reactive support fuels in conjunction with ammonia-based fuels. In 1967, Verkamp et al. [18] found that with $28\%_{vol}$ hydrogen addition to AA, to simulate pre-combustion thermolysis of the ammonia, AA adopted many of the combustion characteristics of conventional fuels. Hydrogen addition increases the S_L of ammonia [1].

A number of related studies have taken place at Cardiff University's Gas Turbine Research Centre investigating hydrogen and methane as potential support fuels for ammonia combustion [20–24]. With the use of these support fuels, premixed swirling flames were established across a narrow range of operable equivalence ratios (Φ). The same premixed, model GT combustor was employed for this experimental campaign.

As with hydrogen addition, fuel/air preheating also increases reactivity and consequently the S_L of ammonia blends. Preheating has been shown to improve efficiencies by decreasing unburned fuel concentrations [25]. However, excessive preheating increases thermal NO_x production.

This work follows on from a detailed numerical study (see [28]) utilizing Chemkin-Pro, which used the ammonia/methane compatible mechanisms of Tian et al. [29] and Okafor et al. [26] for 1-D S_L simulations and for predicting emissions in a 1-D reactor network model. The reactor network comprised a cluster of three perfectly-stirred reactors representing ignition, central recirculation and flame zones, followed by a plug flow reactor for modeling the post flame zone. For atmospheric pressure, an inlet temperature of 550 K was predicted as sufficient for aiding reactivity whilst minimizing thermal NO_x formation, which would result from higher inlet temperatures.

With an inlet of 550 K, the addition of approximately $15\%_{vol}$ COG was numerically found to optimally balance improvements in performance against the production of nitric oxide (NO), carbon monoxide (CO) and ammonia (NH_3) in both the aqueous and AA fuels [28]. As COG is often produced in amounts exceeding its utilization and subsequently flared [11, 30], it is ideal for blending to enhance NH_3 combustion.

NO_x formation in nitrogen-rich fuels can reach levels far greater than equilibrium, as formation is more closely related to kinetics (fuel NO_x) than peak temperatures (thermal NO_x) [27], in contrast to conventional natural gas. Fuel-rich combustion is an effective method for limiting NO_x formation, thus staged combustion has been shown to have the potential to lower overall NO_x emissions [13, 27, 31, 32]. In staged combustion, a fuel-rich stage, consuming the majority of the fuel, is followed by a secondary fuel-lean stage, completing the combustion process, consuming primarily unreacted H_2. High levels of unburned NH_3 entering the lean stage greatly increases overall NO for the system [19, 32].

Experiments by Pugh et al. [22], utilizing the same model GT combustor as used in this study, showed that steam addition has the potential to lower NO_x emissions concentrations in premixed NH_3/H_2 swirling combustion. Thus, the water component, in an AA/AqAV blend, could potentially lower the NO_x emissions concentrations when compared with AA alone.

2. EXPERIMENTAL INVESTIGATION

As in the simulations, the target experimental inlet temperature and operating pressure for the premixed fuel and air

were 550 K and 0.1 MPa respectively. Fuel flow rates equivalent to 25 kW power (LHV) were used for all mixtures.

As previously shown in Fig. 2, AqAV contains trace H_2S, HCN and CO_2. These components were discounted and a surrogate AqAV was formulated composed of 38.35%$_{vol}$ NH_3 and 61.65%$_{vol}$ water vapor. This formulation increased the amount of NH_3 to compensate for the loss of heating value resulting from the absence of H_2S and HCN, and increased the water component to replicate the specific heat capacity of the missing inert CO_2. The delivery of the surrogate AqAV was achieved by combining a preheated air/steam line with anhydrous ammonia (and COG) in the mixing plenum, upstream of the burner.

To reduce costs, the COG composition used for the experimental work was slightly different to the representative COG, as derived from literature and used in the numerical modeling. Table 1 shows the relative compositions, with the experimental blend lacking only the combined 2.2%$_{vol}$ of ethene (C_2H_4) and ethane (C_2H_6).

On a mass basis, experimental COG and that derived from the literature had LHVs of 39.9 and 40.6 MJ/kg respectively.

TABLE 1. COMPARISON OF THE COG COMPOSITION USED EXPERIMENTALLY WITH THAT DERIVED FROM THE LITERATURE

COG Composition	Mole Fractions of Component Gases						
	H_2	CH_4	CO	N_2	CO_2	C_2H_4	C_2H_6
Literature	0.608	0.242	0.07	0.039	0.019	0.017	0.005
Experimental	0.61	0.26	0.07	0.04	0.02	0	0

2.1 Rationale for 50:50%$_{vol}$ AA/AqAV blend

Figure 3 shows numerical simulation results for S_L of AA with 15%$_{vol}$ COG, at a proposed optimal range of Φ and an inlet temperature of 550 K, using the Okafor et al. mechanism [26]. This optimal range (shaded points) reflects a narrow range of Φ where reactor network modeling shows both NO and NH_3 emissions can be simultaneously minimized in the primary stage of staged combustion.

Within the optimal range, the S_L of AA with 15% COG was found to be close to that of very lean methane combustion, using the GRI-Mech 3.0 mechanism [33]. This suggests an AA with 15% COG blend may be capable of stable flames in existing natural gas combustors. However, the AqAV with 15% COG blend failed to reach similar simulated S_L, suggesting that stabilizing the flame could be particularly challenging for this mix.

Combining AA with AqAV, mimicking an effective reduction of water in AqAV, is therefore suggested to increase S_L and further help to stabilize the flame. Figure 3 shows the improvement in simulated S_L for a 50%$_{vol}$ AA to 50%$_{vol}$ AqAV i.e. 50:50 blend, over that of AqAV under the same inlet conditions and COG percentage. Shaded points on this line represent an anticipated optimal operating range of Φ given those predicted for the uncombined ammonia-based fuels.

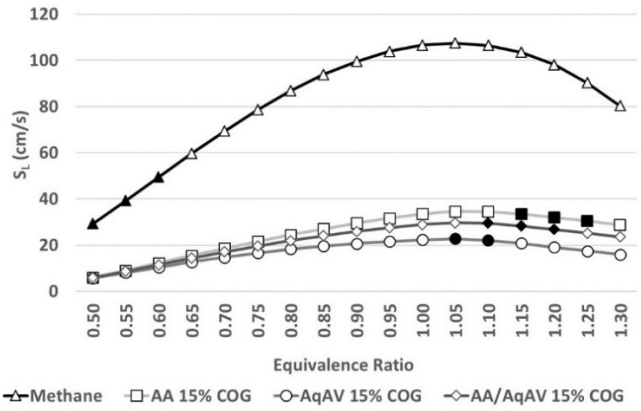

FIGURE 3. S_L AS A FUNCTION OF Φ FOR AA, AqAV AND 50:50%$_{vol}$ AA/AqAV WITH 15%$_{vol}$ COG AND PURE METHANE (550 K, 0.1 MPa)

Other potential benefits result from combining the two ammonia sources, not all related to combustion performance. For example, when using the 50:50 AA/AqAV blend:

- The water in the AqAV fraction increases the mass flow compared with using AA alone, increasing the power generation potential.
- By taking advantage of the move to green ammonia power generation, the opportunity exists to recover the energy potential of ammonia and hydrogen cyanide in industrial waste streams. This is often lost through destruction without energy recovery.
- The same industries that produce by-product ammonia also produce potential hydrogen and/or methane containing support fuels such as COG, biogas and syngas. This gives these industries the potential to act as ammonia power generation 'hubs' to which green AA could be transported.
- Combining AA and AqAV delivers an increase in the potential scale of operation over that of green ammonia alone. Increased scale can lead to efficiency and emissions improvements (e.g. the justification of 'bottoming' cycles and investment in NO_x abatement technologies).

Thus, this study aims to select combined (AA with AqAV) and uncombined (AA or AqAV) blends which optimize the primary fuel-rich stage by simultaneously minimizing NO and NH_3 emissions, under the conditions modeled. These blends must also be found capable of stable combustion. A further aim is to compare cycle efficiencies and net power generated by the selected blends in an Aspen Plus simulated cycle, investigating possible scenarios for ammonia-based fuels utilization.

To represent a 50:50 blend of AA with AqAV, the water component was approximately halved, giving a 70%$_{vol}$ NH_3 to 30%$_{vol}$ H_2O mix.

Target Φ values studied were ±0.05 either side of the optimal ranges for each blend (at 0.05 intervals). This gave an experimental Φ range of 1.0 to 1.15 for AqAV/COG and 1.05 to 1.3 for AA/COG. For the 50:50 AA/AqAV blend with COG, Φ values between 1.0 and 1.2 were studied.

As previously stated, numerical modeling suggested 15% COG addition is optimal for both AA and AqAV. To verify this, 10, 15 and 20%$_{vol}$ COG addition was investigated for each of the three ammonia-based fuels, giving 9 potential fuel blends in total. All blends are described on a volumetric (molar) basis.

2.2 Experimental setup

As in previous studies, a premixed generic swirl burner with a geometric swirl number of 0.8 was employed [22–24]. The burner assembly, shown in Fig. 4, is representative of a typical industrial gas turbine. The 18 mm OD instrumentation lance (Fig. 4a) provides a bluff body stabilization location and temperature measurement within the swirl burner exit nozzle (Fig. 4d). The premixed, preheated air and fuel enter the inlet plenum (Fig. 4b) and proceed to the mixing plenum (Fig. 4c) immediately upstream of the swirl burner. The burner exit is contained within an open-ended cylindrical quartz tube confinement (Fig. 4e), 100 mm in diameter and 385 mm in length, housed inside a pressure casing (Fig. 4f). The expansion ratio of the confinement's internal diameter to the internal diameter of the burner exit nozzle is 2.5. The pressure casing is fitted with quartz windows (Fig. 4g) for non-intrusive, optical observations of the flame structure in the axial plane. The use of this pressure vessel eliminates any atmospheric dilution of the exhaust emissions and will be used for the pressurized combustion experiments in the future.

Steam delivery was achieved by siphoning pressurized water from a Millipore 20 L pressure vessel, into a 24 kW electric heat exchanger in a 'double pass' arrangement. The water flow was regulated using a coriolis mass flow controller (MFC). An electric heat trace was used to maintain heat gains between passes and between the outlet from the heat exchanger to the insulated, preheated air line where the water was injected as steam at atmospheric pressure.

The plenum and burner inlet were preheated to the specified temperature between 502 and 533 K using inline air heaters, which also preheated the fuel. This was used to simulate heat exchange from the exhaust to the fuel/air premix using a recuperator.

As with the water, flow rates for ammonia vapor and COG were also remotely controlled via coriolis MFCs. Air flow was controlled using proportional valves and measured with a coriolis meter.

2.3 Gas analysis method

Approximately 200 mm downstream of the quartz tube exit, a nine-hole equal-area gas analysis probe is situated centrally within the flow of the combustion products. Sampled gases are water-cooled to 433 K in the probe, in accordance with ISO 11042 [34]. The sampled gases are filtered, electrically heated to maintain 433 K as the sample is delivered to the gas analyzers, preventing any components cooling below their respective dew points.

Due to the fuel-rich combustion conditions and the presence of carbon in the COG feed, CO concentrations were especially high and hence, the readings were out of range. To overcome this issue, dry dilution air was added to the sampled product gases, lowering the concentrations to within the measurement range. The fuel-rich combustion and continuous presence of CO in the products allowed for the assumption that all oxygen present in the diluted sample was contributed by the dilution air and not by reactants. The percentage oxygen present in the products was continuously logged. This logged data, when compared to the pre-test ambient average oxygen concentration, was used to calculate dilution values for each experimental condition.

CO_2, CO and O_2 were passed through a chiller and analyzed dry in a Signal 9000MGA multi gas analyzer. CO_2 and CO were measured using a non-dispersive, infrared analyzer, while O_2 was measured using a paramagnetic sensor.

NO was analyzed hot and wet in a Signal 4000VM heated vacuum chemiluminescence analyzer, so the readings required normalization to dry equivalent conditions. The product water fraction was taken from equilibrium modeling for each case. The NO_x analyzer has an accuracy of > ±1% of range.

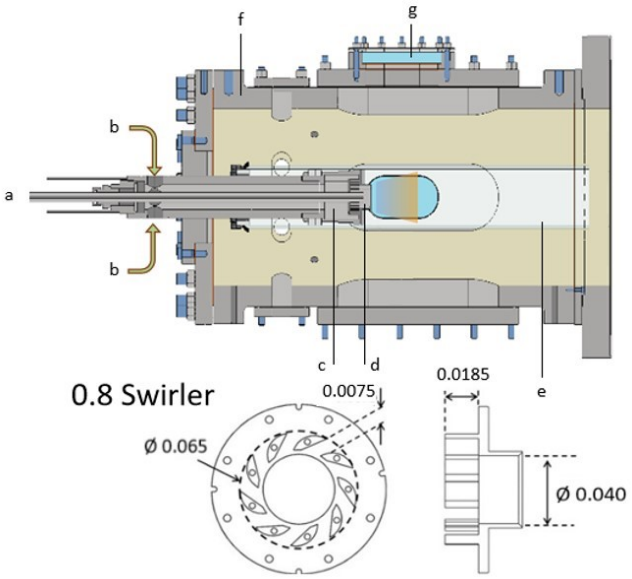

FIGURE 4. CROSS-SECTION OF GENERIC SWIRL BURNER ASSEMBLY AND GEOMETRY OF THE SWIRL BURNER (DIMENSIONS IN METERS)

Ammonia was reacted with O_2 at 1023 K, over a platinum on alumina catalyst, in a Signal 410 ammonia converter. The NO (and water vapor) product was sent to the NO analyzer and was analyzed wet in the same manner as the NO previously mentioned. The system allowed samples to be exchanged between the direct feed from the gas probe and the outlet of the ammonia converter. Readings for NO and NH_3 were therefore taken alternately for each experimental condition, the direct NO readings being subtracted from those including the converted ammonia, allowing for the conversion efficiency of 81% (as found during analyzer calibration). Fluctuations in air dilution were considered by recording oxygen concentrations for each of the NO and ammonia sampling periods separately within each

condition. All figures show the precise experimental Φ as derived from the data.

After accounting for dilution, all emissions concentrations were calculated as dry, and referenced to 15% excess O_2, as per the regulatory requirements for GT technology in the European Union [35]. NO_2 is not included for simplicity, as it is considered consistently scaled to NO and a minor component of NO_x in ammonia combustion.

3. EXPERIMENTAL RESULTS AND DISCUSSION

Due in part to the low air flows required for ammonia combustion, especially under fuel-rich conditions, the air preheat limited the operating temperatures to between 502 and 533 K with the lower inlet temperatures tending to occur at higher Φ. Combustor inlet pressure was 0.109 MPa.

The AqAV/COG readings could only be taken for 20% COG addition. The AqAV with 15% and 10% COG were too unstable or incapable of sustaining a viable flame. This agrees with predictions based on the low S_L for the AqAV blends under these conditions (see Fig. 3). For 20% COG, at Φ = 1.15, the flame structure underwent frequent transition. Likewise, the flame for AA/AqAV with 10% COG at Φ = 1.2, was too unstable for safe operation, lifting off the burner. It is expected that an increased inlet temperature (~550 K) would enable stable operation at this condition as suggested by the kinetic modeling.

3.1 Carbon monoxide (CO) emissions

As expected, CO emissions increased significantly with increasing Φ. As Fig. 5 shows, CO emissions are marginally higher for the AA/AqAV blends than the AA blends. This increase in unburned fuel concentrations is due to the presence of water lowering the reactivity, e.g. the adiabatic flame temperature (AFT) and S_L, of the AA/AqAV blends.

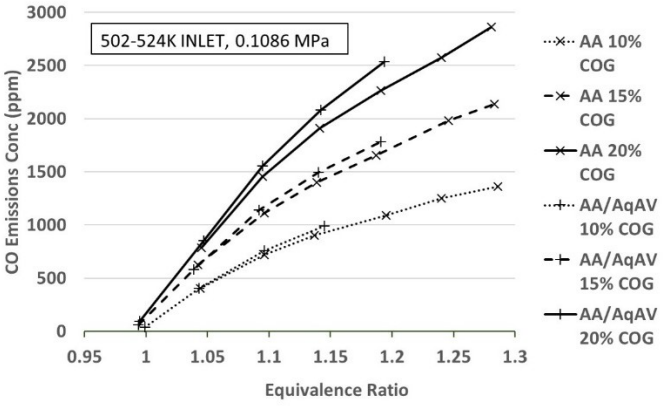

FIGURE 5. CO EMISSIONS BY EQUIVALENCE RATIO FOR AA AND AA/AqAV WITH 10, 15 AND 20%$_{vol}$ COG (DRY, 15% O_2)

The excessive CO concentrations highlight the need for a subsequent lean stage, to complete CO burnout. Naturally, CO emissions are higher for the mixes with higher percentages of COG, due to the increased CH_4 component.

3.2 Nitric oxide (NO) and ammonia (NH_3) emissions

In the flame zone, fuel bound nitrogen reacts rapidly with oxygen to produce NO. With less air at higher Φ, concentrations of unburned fuel are higher and the reactivity of the fuel/air mix is lower. Unburned ammonia dissociates into amine radicals NH_2, NH and N which react with NO to form water and N_2. This is why NO concentrations decrease with increasing Φ, as shown in Figs. 6, 7 and 8.

Similarly, less supporting fuel lowers mix reactivity. Thus, less COG results in more unburned ammonia to react with NO, explaining why NO concentrations are lower and NH_3 concentrations generally higher with less COG.

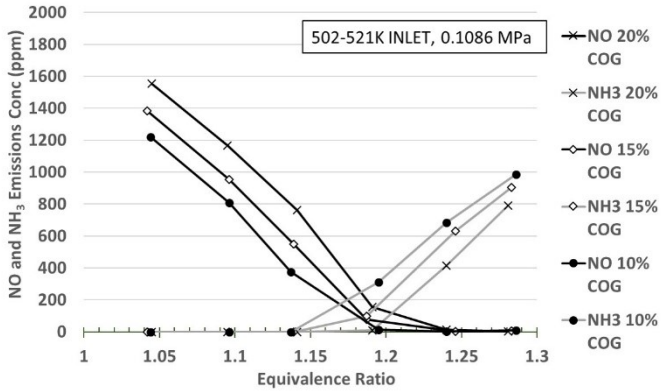

FIGURE 6. NO AND NH_3 EMISSIONS BY EQUIVALENCE RATIO FOR AA WITH 10, 15 AND 20%$_{vol}$ COG (DRY, 15% O_2)

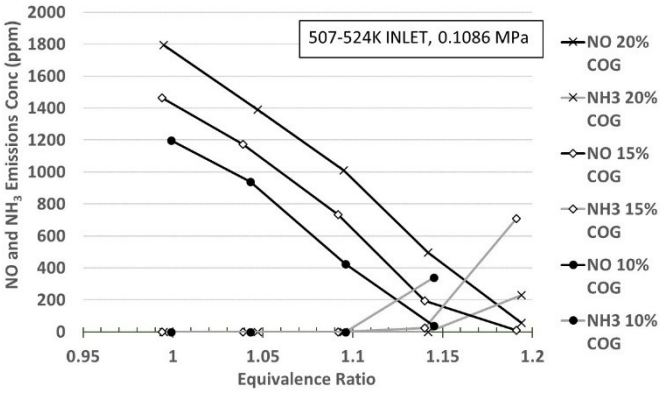

FIGURE 7. NO AND NH_3 EMISSIONS BY EQUIVALENCE RATIO FOR 50:50%$_{vol}$ AA/AqAV WITH 10, 15 AND 20%$_{vol}$ COG (DRY, 15% O_2)

The AA blends (Fig. 6) have higher NO concentrations than the equivalent AA/AqAV blends at the same Φ. This is because the addition of water reduces the flame temperature and reactivity of the AA/AqAV blends.

Without preheating, thermal NO has been found negligible compared to fuel NO in ammonia combustion [36]. However, increasing burner inlet temperature and supporting fuels percentage, enhances the role of thermal NO. Therefore, some of the reduction in NO with lower reactivity is due to lower AFT, reducing thermal NO_x production.

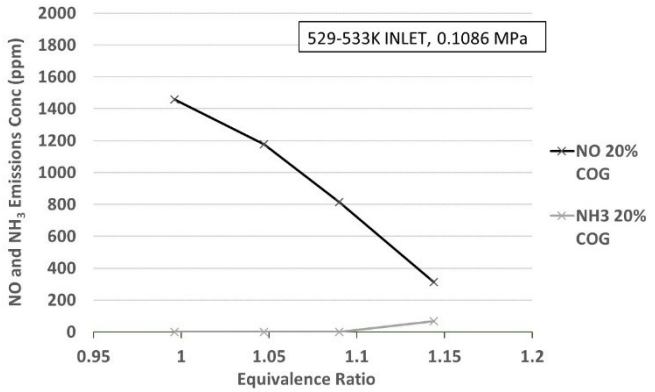

FIGURE 8. NO AND NH_3 EMISSIONS BY EQUIVALENCE RATIO FOR AqAV WITH 20%$_{vol}$ COG (DRY, 15% O_2)

Thus, NO emissions decrease with increasing Φ and NH_3 emissions increase substantially above a certain value of Φ for each fuel mixture (see Figs. 6 and 7). NH_3 emissions must be minimized before the lean second stage to avoid high rates of NO production at Φ < 1 [19].

At Φ = 1.187, the AA with 15% COG blend had its lowest combined NO and NH_3 readings of 174 ppm (76 and 98 respectively). The 20% COG blend was also capable of a similar lowest combined reading of 162 ppm for NO and NH_3 (155 and 7 respectively) at Φ = 1.191. The 15 and 20% COG blends exhibited improved combined emissions performance over the 10% COG blend. Given the similar values for lowest combined NO/NH_3 emissions in the 15 and 20% COG blends, the 15% COG blend was selected for the cycle analysis, due to the lower requirement for carbon-containing support fuel.

The lowest combined NO/NH_3 reading for the AA/AqAV with 15% COG blend, was obtained at Φ = 1.140. This combined reading of 219 ppm (196 ppm NO and 23 ppm NH_3) was less than the lowest combined measure for the AA/AqAV with 20% COG blend, which was 283 ppm (54 ppm NO and 229 ppm NH_3) at Φ = 1.194. Once again, the more unstable nature of the 10% COG flame, favors the other two AA/AqAV blends. The lower requirement for carbon-containing support fuel, lower combined emissions and far lower unburned NH_3 leaving the primary stage, makes the AA/AqAV with 15% COG the leading AA/AqAV blend for cycle analysis.

Based on these measurements, the AA/AqAV blends are less favorable than the equivalent AA blends due to their higher combined emissions, showing that despite lower NO at the same Φ, water addition does not guarantee lower combined emissions overall.

Experimental results were used to improve heat losses, recirculation ratios and residence times for the reactor network model described in Section 1.3. Heat losses and residence times in perfectly-stirred reactors 1 to 3 were 0.1 kW/0.001 s, 0.8 kW/0.005 s and 0.8 kW/0.02 s respectively. Recirculation between reactors was modified to 30%. Heat loss in the plug flow reactor was modeled for 0.3 kW/cm. The improved reactor network model was used to predict H_2 concentrations as a fraction of all products leaving the primary combustor. For AA with 15% COG (Φ = 1.2) and AA/AqAV with 15% COG (Φ = 1.15) predicted H_2 concentrations were 5.1 and 3.7%$_{vol}$ respectively.

3.3 Optimizing Φ using laminar burning velocity

The equivalence ratio was varied by 0.05, which does not necessarily capture NO/NH_3 emissions at their absolute minimum. An optimal Φ, or Φ_{opt}, whereby both NO and NH_3 can be simultaneously minimized for each blend, is reached when NH_3 and NO concentrations are equal.

The values of Φ_{opt} taken from Figs. 6 and 7 (to the nearest 0.005) are shown in Table 2. Also in Table 2, the S_L for each blend at its Φ_{opt} has been simulated using the Okafor et al. mechanism [26] in Chemkin-Pro. Temperatures and pressures used in the simulations are those of the experimental condition nearest to each blends' Φ_{opt}.

The results in Fig. 9 use the values in Table 2 to show a strong positive linear correlation for Φ_{opt} against S_L for the six AA and AA/AqAV blends. A trend line passes through, or near, the six points and is then extrapolated (dotted trend line). This trend is useful for predicting which values of Φ_{opt} are likely for any similar blend by modeling its S_L. This trend was not identified when correlating Φ_{opt} with AFT.

TABLE 2. Φ_{opt} FOR BLENDS AND THEIR RESPECTIVE LAMINAR BURNING VELOCITIES

Fuel		P (MPa)	Inlet T (K)	Φ_{opt}	S_L (cm/s)
COG %	Ammonia				
20% COG	AA	0.1088	512.5	1.205	29.157
15% COG	AA	0.1088	506.3	1.185	26.461
10% COG	AA	0.1089	507.4	1.170	24.623
20% COG	AA/AqAV	0.1086	506.8	1.180	24.946
15% COG	AA/AqAV	0.1085	513.3	1.150	23.078
10% COG	AA/AqAV	0.1084	515.3	1.125	20.577

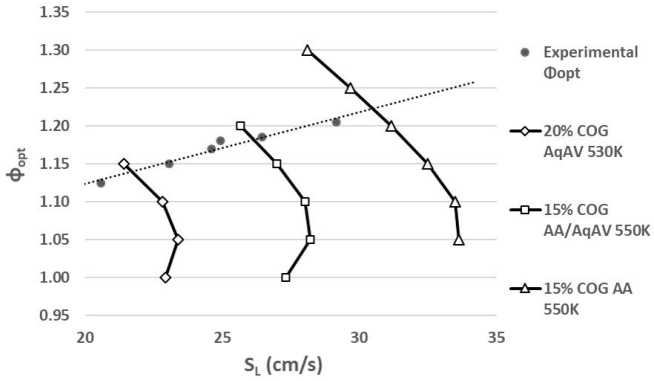

FIGURE 9. EXPERIMENTALLY DERIVED Φ_{opt} AGAINST MODELED S_L FOR SELECTED FUEL BLENDS

Laminar flame speed for AqAV with 20% COG over the range of Φ and at the same experimental conditions, are also

plotted in Fig. 9. This line intersects the trend line for Φ_{opt} at an approximate Φ_{opt} of 1.13. As emissions for NH_3 and NO were not minimized at $\Phi = 1.13$ (see Fig. 8) combustion instabilities may be responsible. Combustion instabilities were considerable at $\Phi = 1.15$, so operation at $\Phi = 1.13$ was impractical. Thus, the AqAV with 20% COG blend was too unstable for further investigation.

The other two lines in Fig. 9 represent the modeled S_L values for the two leading AA and AA/AqAV blends at 550 K inlet, for the Φ range tested. Assuming the trend is robust across inlet temperature changes, at 550 K the Φ_{opt} for each blend will increase. The AA and AA/AqAV with 15% COG blends would have Φ_{opt} values ~1.22 (previously ~1.185) and ~1.18 (previously ~1.15) respectively.

3.4 Reactor network modeling at increased pressure

The improved reactor network model was used to predict the effect of increased pressure on Φ_{opt} in the primary stage. Inlet flows were scaled for 1.2 MPa for the two leading blends, to match the pressure ratio of the cycle analysis used in Section 4. Figure 10 shows the experimental results at atmospheric pressure and also modeled results (Okafor et al. mechanism) for atmospheric and 1.2 MPa pressure, for the leading AA blend, using the experimental inlet temperature. Emissions concentrations are given as wet. Modeling shows that at increased pressure, stable combustion is anticipated and both NO and NH_3 concentrations are predicted to decrease considerably and be less sensitive to changes in Φ. Similar findings were indicated for the leading AA/AqAV blend.

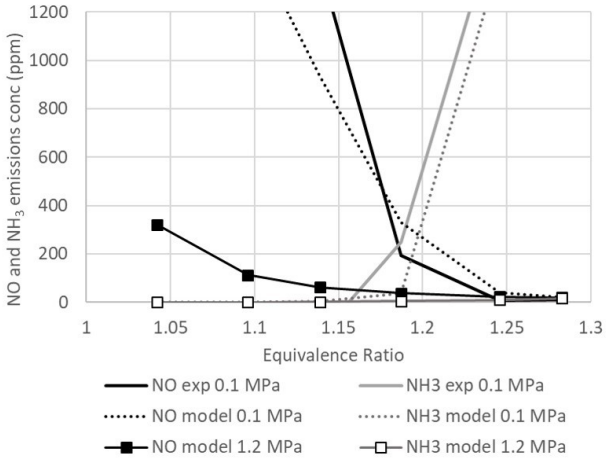

FIGURE 10. NO AND NH_3 EMISSIONS BY EQUIVALENCE RATIO FOR AA WITH 15%$_{vol}$ COG WITH VARYING PRESSURE

4. CYCLE INVESTIGATION USING ASPEN PLUS

To gauge an approximate power output from the two leading experimental mixes, a simulated steady state thermodynamic cycle has been developed using Aspen Plus. Much of the cycle arrangement and many of the settings are the same as those used in the published preparatory study. Important settings not displayed in Fig. 11, are summarized in Table 3. The reader is referred to the previous study for further details and explanations [28]. All simulations fully converged.

TABLE 3. ASPEN PLUS THERMODYNAMIC CYCLE SETTINGS

Brayton Cycle	
GT efficiency	isen. 90% : mech. 99%
GT exit T (all cases)	873 K
Compressor efficiency	isen. 88% : mech. 99%
Recuperator min. T approach	30 K
Rankine Cycle	
Final condensation T	293 K
HRSG exhaust T (all cases)	393 K
Steam Turbine Efficiency	isen. 90% : mech. 99%
Pump efficiency	80% overall
Pump pressure	10 MPa
Property Methods etc.	
Brayton cycle	Peng-Robinson
Rankine cycle	IAPWS-95
Air composition	78% N_2 : 21% O_2 : 1% argon

The cycle consists of a Brayton cycle, followed by a Rankine bottoming cycle. Heat transfer from the compressed air alone is insufficient to both vaporize the ammonia and achieve the required preheat to aid reactivity in the fuel/air mix. Although waste heat on site could be used to preheat the inlet, the Brayton cycle incorporates the use of a recuperator, preheating the air/fuel mix to 550 K, for a self-sustaining cycle. Although the likelihood of incorporating a Rankine cycle would naturally depend on the scale of operation, it is included to enable easy comparison with efficiencies of contemporary combined cycles.

This analysis focuses on the potential benefits of combining green ammonia with industrial waste stream ammonia, supported by 15%$_{vol}$ COG (due to the experimental results), in three practical scenarios. As steelworks industrial waste stream ammonia is only practically available as either recovered anhydrous or ~60% aqueous, achieving an ammonia feed with a 30% steam content requires combining an anhydrous source, e.g. green ammonia, with the aqueous stream in a fixed ratio (i.e. 50:50). The inlet mass flows for the three scenarios are scaled to the availability of 10 tonnes of by-product ammonia/day.

4.1 Outline of Aspen Plus cycle scenarios

The scenarios assume 15% COG blending and are summarized in Table 4:

1. Green ammonia is imported and augmented with AqAV in a 50:50 blend (simplified to 70% NH_3, 30% H_2O - as tested experimentally).
2. Industrial NH_3 recovered from AqAV as 10 tonnes/day of AA, (e.g. using the PHOSAM process).
3. The same amount of green ammonia as for scenario 1, without the addition of AqAV to highlight the difference when not augmenting the green ammonia with AqAV.

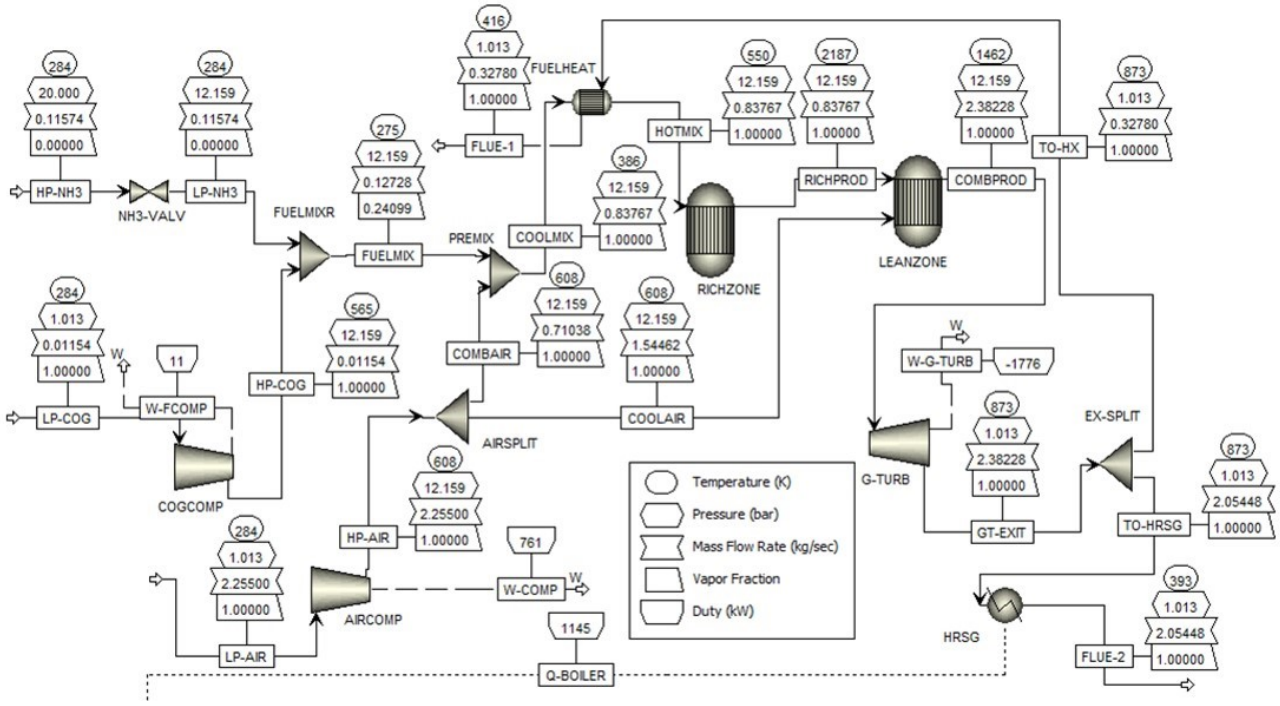

FIGURE 11. SCENARIO 2: 85% ANHYDROUS AMMONIA/15% COG, BRAYTON CYCLE WITH RECUPERATOR AND HRSG

TABLE 4. SCENARIOS FOR AMMONIA-BASED FUEL CYCLE

Scenario	Representative Ammonia Fuel	Green Ammonia (tonnes/day)	NH_3 in AqAV (tonnes/day)	Φ_{opt}
1	50:50 AA/AqAV	25	10	1.15
2	AA	0	10	1.2
3	AA	25	0	1.2

In the simplified 50:50 AA/AqAV blend, AqAV contains 40% NH_3. This 40% has a mass flow of 10 tonnes/day. Therefore, the ammonia component of AqAV represents 28.6% of the mass of all the ammonia in a 50:50 AA/AqAV blend. Thus, the total mass flow of NH_3 into this cycle would be 35 tonnes/day. Approximate values of Φ_{opt} for the blends in the primary stage of combustion are given in Table 4. Precise values are not important for the thermodynamic cycle as the fuel is assumed to be completely consumed in the second stage. Figure 11 shows the modeled Brayton cycle with recuperator, as applied to scenario 2 with no combustor losses. Naturally, as flow rates of the ammonia-based fuels increase, the demand for COG, as a fixed 15%$_{vol}$ of the overall composition, also increases. This is partly responsible for the increases in net power with higher flow rates of ammonia.

4.2 Cycle summary

A pressure reducing valve for the ammonia-based fuel, plus compressors for the COG and air feeds, supply a pressure of ~1.2 MPa to the combustion chamber. This pressure ratio is typical for GTs in the ~5 MW scale [37]. The air compressor supplies combustion air to both the primary fuel-rich stage 'RICHZONE' and the secondary lean stage 'LEANZONE'.

The air splitter 'AIRSPLIT' ensures the primary reactor 'RICHZONE' is fed the amount of air to achieve the Φ_{opt} for each of the blends (see Table 4). The primary combustion air, heated by the compressor, is combined with the fuel mix in the mixer 'PREMIX'. Before entering the combustor, the premixed air and fuel is preheated to 550 K via the return of the minimum required percentage of turbine exhaust to the recuperator. Turbine exhaust not used for recuperation proceeds to a heat recovery steam generator (HRSG), which provides heat to the Rankine cycle (dotted line). The 'LEANZONE' reactor is fed with the remaining air from 'AIRSPLIT', which completes the combustion of the unburned fuel from the primary stage and cools the combustion products upstream of the turbine.

Both reactors are equilibrium reactors. This type of reactor is based on minimizing Gibbs free energy and is typically used for combustion and similar complex reaction simulations in Aspen Plus. Unlike with conventional gaseous fuels, the formation of NO_x for fuels that contain nitrogen, such as ammonia, is far more dependent on kinetics than equilibrium. Aspen Plus is not compatible with the complex reaction mechanisms developed for modeling NO_x formation in ammonia combustion, therefore Chemkin-Pro is used for modeling emissions (as in the preparatory study). Regardless, the effect on thermodynamic data, due to differences in modeling via equilibrium or kinetics for complete combustion of ammonia, is negligible.

As the cycle is conceptual, heat and pressure losses from the combustor were modeled for no losses (adiabatic), 5%, 10%, 15% and 20% of LHV to indicate the impact of combustor losses on the overall power and efficiency of the cycle.

5. ASPEN PLUS CYCLE RESULTS AND DISCUSSION

As Fig. 12 shows, the AA scenarios, i.e. 2 and 3, are more efficient overall than scenario 1 and, as the only difference is in scale of operation, they have the same efficiency.

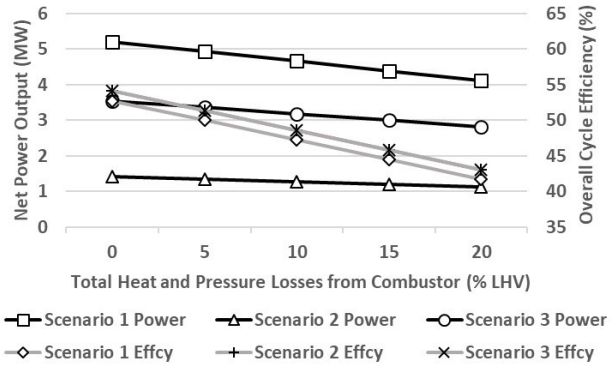

FIGURE 12. COMBINED CYCLE NET POWER AND EFFICIENCY AGAINST COMBUSTOR LOSSES FOR SCENARIOS 1 TO 3

Cycle efficiencies are based on fuel LHVs, as is the convention in combined cycle gas turbine efficiency values. At 10% combustor losses, the overall efficiencies of the AA with COG and the AA/AqAV with COG cycles are 48.6% and 47.3% respectively.

The overall efficiency of scenario 1 is lower because a higher percentage of the exhaust flow, 26.7% at 10% combustor losses, is used in the recuperator to achieve the 550 K inlet temperature, leaving less exhaust heat for the Rankine cycle. Equivalent exhaust flow to the recuperator is 15.3% for scenarios 2 and 3.

Net electrical power available from scenarios 1, 2 and 3 (at 10% combustor losses) is 4.7, 1.3 and 3.2 MW respectively, indicating an additional ~1.5 MW from the addition of industrial AqAV/COG to the green ammonia/COG. Utilizing the AqAV (and its allied COG) has improved the generating capacity of the green ammonia/COG by ~47%. This significant improvement in generating capacity supports the case for transporting green ammonia for co-firing with AqAV and COG.

Scenario 2, AqAV processed to AA, only generates 1.3 MW, so less than the ~1.5 MW enhancement when using AqAV unprocessed. Processing AqAV into AA incurs additional energy, materials and infrastructure costs ahead of combustion. These costs are not factored here, but clearly would be detrimental to the cycle efficiency if included, further highlighting the benefit of using AqAV unprocessed.

Figure 13 shows that, when excluding the Rankine cycle, the cycle efficiency situation is reversed. The addition of AqAV to green ammonia increases the efficiency from 34.6% to 35.1% (at 10% combustor losses).

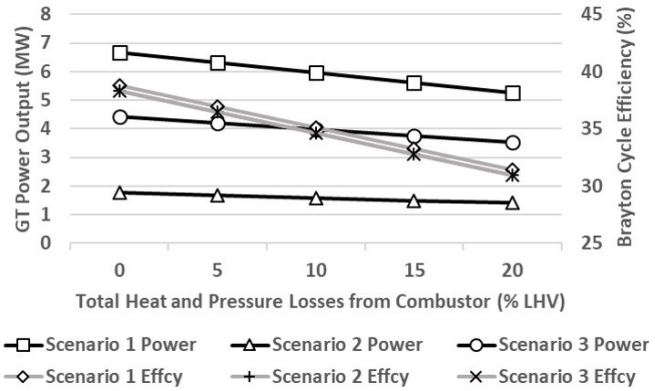

FIGURE 13. GT POWER AND BRAYTON CYCLE EFFICIENCY AGAINST COMBUSTOR LOSSES FOR SCENARIOS 1 TO 3

The sizing of the GT is ~2 MW greater in scenario 1 than 3. Larger GTs are inherently more efficient, so in reality, this differential would likely be greater. GTs of this scale do not justify the inclusion of bottoming cycles. Thus, for Brayton only cycles, efficiencies are maximized when adopting scenario 1, combining AA with AqAV.

6. CONCLUSIONS AND FURTHER WORK

This study has found experimentally that it is possible to combust 15% COG with both AA and a 70% AA, 30% water blend, to achieve a stable flame in a swirl burner using >500 K preheat at atmospheric pressure. Also, under these conditions and at the approximate Φ_{opt}, NO and NH_3 emissions can be minimized to combined levels of <200 ppm and <300 ppm for the AA and AA/AqAV (with $15\%_{vol}$ COG) blends respectively. Further work is required to resolve the Φ_{opt} for the blends, to predict the ideal fuel-rich primary zone operating conditions. Trends indicate that Φ_{opt} correlates positively and linearly with S_L for these mixes.

Cycle analysis shows that under typical system losses, combined cycle efficiencies of almost 50% are achievable for these blends, potentially higher if reactants are preheated via the utilization of waste heat on a steelworks site.

Without a bottoming cycle, AA/AqAV with COG achieves marginally higher efficiencies than AA with COG with efficiencies for both of ~ 35%. Given the scale of operation, i.e. ~6 MW, this is the likely configuration for a modest-sized steel plant.

Transporting green ammonia to a steelworks site enables the use of COG as a support fuel. When augmented with ammonia from industrial wastewater, net power is increased by ~47%. This increase promotes and potentially enables the earlier uptake of green ammonia to power projects.

The next stage of investigation will be to experimentally verify Φ_{opt} with change in inlet temperature, for the two leading blends, followed by the optimization of staged combustion to replicate the combustor in the cycle modeled in Aspen. Furthermore, the effects of increasing burner pressure on operability, emissions and Φ_{opt} will be evaluated.

ACKNOWLEDGMENTS

The first author is funded through an EPSRC PhD Studentship. The project is also supported by FLEXIS (Flexible Integrated Energy Systems) a research project designed to develop energy-systems research capacity in South Wales.

The authors would also like to thank Mr. Steve Morris, facility manager at the Cardiff University Gas Turbine Research Centre, for his significant technical input and dedication to this work and technician Jack Thomas, for his help in setting up the experimental study.

REFERENCES

[1] Valera-Medina, A., Xiao, H., Owen-Jones, M., David, W. I. F., and Bowen, P. J. "Ammonia for power." *Progress in Energy and Combustion Science* Vol 69 (2018): pp. 63-102. DOI:10.1016/j.pecs.2018.07.001.

[2] Ahlgren, W. L. "The dual-fuel strategy: an energy transition plan." *Proceedings of the IEEE* Vol. 100 No. 11 (2012): pp. 3001–3052. DOI:10.1109/JPROC.2012.2192469.

[3] Wilkinson, I. "The Role of "Green" Ammonia in Decarbonising Energy Systems: Practical Demonstration and Economic Considerations." *NH3 Fuel Conference*, Minneapolis (2017).

[4] Giddey, S., Badwal, S. P. S., Munnings, C. and Dolan, M. "Ammonia as a Renewable Energy Transportation Media." *ACS Sustainable Chemistry & Engineering* Vol. 5 No. 11 (2017): pp. 10231–10239. DOI:10.1021/acssuschemeng.7b02219.

[5] Djinović, P. and Schüth, F. "Energy carriers made from hydrogen." P. and G. Moseley (Ed.) *Electrochemical Energy Storage for Renewable Sources and Grid Balancing* (2014): pp. 183–199. DOI:10.1016/B978-0-444-62616-5.00012-7.

[6] Zamfirescu, C. and Dincer, I. "Using ammonia as a sustainable fuel." *Journal of Power Sources* Vol. 185 No. 1 (2008): pp. 459–465. DOI:10.1016/j.jpowsour.2008.02.097.

[7] U.S. Geological Survey. *Mineral Commodity Summaries 2019.*

[8] Remus, R., Roudier, S., Aguado-Monsonet, M. A. and Delgado Sancho, L. "Best available techniques - iron and steel production." *Industrial Emissions Directive 2010/75/EU* (2013): DOI:10.2791/97469.

[9] Kohl, A. L. and Nielsen, R. *Gas Purification.* Gulf Publishing, Houston (1997).

[10] Worldsteel Association. "World Steel in Figures 2018." from https://www.worldsteel.org/media-centre/press-releases/2018/world-steel-in-figures-2018.html, accessed 4-2-2019.

[11] Razzaq, R., Li, C. and Zhang, S. "Coke oven gas: Availability, properties, purification, and utilization in China." *Fuel* Vol. 113 (2013): pp. 287–299. DOI:https://doi.org/10.1016/j.fuel.2013.05.070.

[12] Bermúdez, J. M., Arenillas, A., Luque, R. and Menéndez, J. A. "An overview of novel technologies to valorise coke oven gas surplus." *Fuel Processing Technology* Vol. 110 (2013): pp. 150–159. DOI:10.1016/J.FUPROC.2012.12.007.

[13] Teng, H. "Combustion modifications of batch annealing furnaces and ammonia combustion ovens for NO_x abatement in steel plants." *Journal of the Air and Waste Management Association* Vol. 46 No. 12 (1996): pp. 1171–1178. DOI:10.1080/10473289.1996.10467552.

[14] Svoboda, K. and Diemer, P. "Catalytic decomposition of ammonia from coke-oven gas." *Iron and Steel Engineer* Vol. 67 No. 12 (1990): pp. 42–46.

[15] Industrial Efficiency Technology Database. "Coke making" from http://ietd.iipnetwork.org/content/coke-making, accessed 1-8-2018.

[16] Worldsteel Association. "Steel and raw materials fact sheet." (2018): from https://www.worldsteel.org/steel-by-topic/raw-materials.html, accessed 1-8-2018.

[17] Ekgauz, V. I., Pokryshkin, K. V., Tretiakova, G. D., Dementieva, N. V., Stepina, L. A., Putilov, A. V., Motovilova, N. K., Ryazanov, O. V., Kalinin, A. V., Blokhin, M. I., Grakhovskiy, A. V. and Sorokina, I. V. "Removal of ammonia from coke-oven gas at PAO Severstal' by a circulatory phosphate method." *Coke and Chemistry* Vol. 59 No. 3 (2016): pp. 92–100. DOI:10.3103/S1068364X16030030.

[18] Verkamp, F. J., Hardin, M. C. and Williams, J. R. "Ammonia combustion properties and performance in gas-turbine burners." *Symposium (International) on Combustion* Vol. 11 (1967): pp. 985–992. DOI:https://doi.org/10.1016/S0082-0784(67)80225-X.

[19] Kobayashi, H., Hayakawa, A., Somarathne, K. D. K. A. and Okafor, E. C. "Science and technology of ammonia combustion." *Proceedings of the Combustion Institute* Vol. 37 No. 1 (2019): pp. 109–133. DOI:10.1016/j.proci.2018.09.029.

[20] Valera-Medina, A., Morris, S., Runyon, J., Pugh, D. G., Marsh, R., Beasley, P. and Hughes, T. "Ammonia, methane and hydrogen for gas turbines." *Energy Procedia* Vol. 75 (2015): pp. 118–123. DOI:https://doi.org/10.1016/j.egypro.2015.07.205.

[21] Valera-Medina, A., Gutesa, M., Xiao, H., Pugh, D., Giles, A., Goktepe, B., Marsh, R. and Bowen, P. "Premixed ammonia/hydrogen swirl combustion under rich fuel conditions for gas turbines operation." *International Journal of Hydrogen Energy* Vol. 44 No. 16 (2019): DOI:10.1016/j.ijhydene.2019.02.041.

[22] Pugh, D., Bowen, P., Valera-Medina, A., Giles, A., Runyon, J. and Marsh, R. "Influence of steam addition and elevated ambient conditions on NO_x reduction in a staged premixed swirling NH_3/H_2 flame." *Proceedings of the Combustion Institute* (2018): DOI:10.1016/j.proci.2018.07.091.

[23] Valera-Medina, A., Marsh, R., Runyon, J., Pugh, D., Beasley, P., Hughes, T. and Bowen, P. "Ammonia–methane combustion in tangential swirl burners for gas turbine power generation." *Applied Energy* Vol. 185 (2016): pp. 1362–1371. DOI:10.1016/j.apenergy.2016.02.073.

[24] Valera-Medina, A., Pugh, D. G., Marsh, P., Bulat, G. and Bowen, P. "Preliminary study on lean premixed combustion of ammonia-hydrogen for swirling gas turbine combustors." *International Journal of Hydrogen Energy* Vol. 42 No. 38 (2017): DOI:10.1016/j.ijhydene.2017.08.028.

[25] Kurata, O., Iki, N., Matsunuma, T., Inoue, T., Tsujimura, T., Furutani, H., Kobayashi, H. and Hayakawa, A. "Performances and emission characteristics of NH_3-air and NH_3-CH_4-air combustion gas-turbine power generations." *Proceedings of the Combustion Institute* Vol. 36 No. 3 (2017): pp. 3351–3359. DOI:10.1016/J.PROCI.2016.07.088.

[26] Okafor, E. C., Naito, Y., Colson, S., Ichikawa, A., Kudo, T., Hayakawa, A. and Kobayashi, H. "Experimental and numerical study of the laminar burning velocity of CH_4-NH_3-air premixed flames." *Combustion and Flame* Vol. 187 (2018): pp. 185–198. DOI:10.1016/j.combustflame.2017.09.002.

[27] Wendt, J. O. L. and Sternling, C. V. "Effect of ammonia in gaseous fuels on nitrogen oxide emissions." *Journal of the Air Pollution Control Association* Vol. 24 (1974): pp. 1055–1058. DOI:10.1080/00022470.1974.10470013.

[28] Hewlett, S. G., Valera-Medina, A., Pugh, D. G. and Bowen, P. J. "Gas Turbine Co-Firing of Steelworks Ammonia with Coke Oven Gas: A Fundamental and Cycle Analysis." *Proceedings of the ASME Turbo Expo* (2019): pp. GT2019-91404. DOI:10.1115/GT2019-91404.

[29] Tian, Z., Li, Y., Zhang, L., Glarborg, P. and Qi, F. "An experimental and kinetic modeling study of premixed NH_3/CH_4/O_2/Ar flames at low pressure." *Combustion and Flame* Vol. 156 No. 7 (2009): pp. 1413–1426. DOI:10.1016/j.combustflame.2009.03.005.

[30] Pugh, D. *Combustion characterisation of compositionally dynamic steelworks gases* Cardiff University PhD Thesis (2013): Retrieved from http://orca.cf.ac.uk/58006/.

[31] Li, S., Zhang, S., Zhou, H. and Ren, Z. "Analysis of air-staged combustion of NH_3/CH_4 mixture with low NO_x emission at gas turbine conditions in model combustors." *Fuel* Vol. 237 (2019): DOI:10.1016/j.fuel.2018.09.131.

[32] Somarathne, K. D. K. A., Hatakeyama, S., Hayakawa, A. and Kobayashi, H. "Numerical study of a low emission gas turbine like combustor for turbulent ammonia/air premixed swirl flames with a secondary air injection at high pressure." *International Journal of Hydrogen Energy* Vol. 42 No. 44 (2017): pp. 27388–27399. DOI:10.1016/j.ijhydene.2017.09.089.

[33] Smith, G. P., Golden, D. M., Frenklach, M., Moriarty, N. W., Eiteneer, B., Goldenberg, M., Bowman, C. T., Hanson, R. K., Song, S., Gardiner, Jr., W. C., Lissianski, V. V., Qin, Z. "GRI-Mech 3.0", from http://www.me.berkeley.edu/gri_mech/, accessed 5-2-2020.

[34] International Organization for Standardization. "ISO 11042-1:1996 - Gas turbines - Exhaust gas emission - Part 1: Measurement and evaluation." from https://www.iso.org/standard/19022.html, accessed 18-11-2019.

[35] European Union. "Directive (EU) 2015/ 2193 of the European Parliament and of the Council on the limitation of emissions of certain pollutants into the air from medium combustion plants." *Official Journal of the European Union EN* Vol. 451 No. 354 (2014): pp. 134–23.

[36] Li, J., Huang, H., Kobayashi, N., He, Z. and Nagai, Y. "Study on using hydrogen and ammonia as fuels: Combustion characteristics and NO_x formation." *International Journal of Energy Research* Vol. 38 No. 9 (2014): pp. 1214–1223. DOI:10.1002/er.3141.

[37] Siemens. "Siemens products and services – energy - power generation - gas turbines" from https://new.siemens.com/global/en/products/energy/power-generation/gas-turbines.html, accessed 6-8-2019.

